Journal of Biomechanics ∎ (∎∎∎∎) ∎∎∎–∎∎∎

Contents lists available at ScienceDirect

Journal of Biomechanics

journal homepage: www.elsevier.com/locate/jbiomech
www.JBiomech.com

Numerical analysis of hemodynamic changes in the left atrium due to atrial fibrillation

Ryo Koizumi [a], Kenichi Funamoto [b,*], Toshiyuki Hayase [b], Yusuke Kanke [a], Muneichi Shibata [c], Yasuyuki Shiraishi [d], Tomoyuki Yambe [d]

[a] Graduate School of Engineering, Tohoku University, Japan
[b] Institute of Fluid Science, Tohoku University, Japan
[c] Miyagi Cardiovascular and Respiratory Center, Japan
[d] Institute of Development, Aging and Cancer, Tohoku University, Japan

ARTICLE INFO

Article history:
Accepted 5 December 2014

Keywords:
Atrial fibrillation
Left atrium
Hemodynamics
Computational fluid dynamics
Magnetic resonance imaging

ABSTRACT

Atrial fibrillation (AF) disrupts movement of the left atrium (LA) and worsens the vital prognosis by causing thromboembolism. Ultrasound Doppler measurement, phase-contrast magnetic resonance imaging (PC MRI), as well as computational fluid dynamics (CFD) have revealed hemodynamic changes in the LA due to AF, such as stagnation of blood flow in the left atrial appendage (LAA). However, quantitative evaluation of the hemodynamics during AF has not been conducted, and the effects of important AF characteristics, such as a lack of active contraction of the LA (atrial kick) in late diastole and the occurrence of high-frequency fibrillation (>400 bpm) of the atrial wall, on blood flow field and concomitant hemodynamic stresses have not been completely understood. In this study, the effects of the above-mentioned two characteristic phenomena of AF on blood flow and hemodynamic parameters were quantitatively investigated. Based on MRI of a healthy volunteer heart, one healthy LA model and two AF models (one without atrial kick, and one without atrial kick and with high-frequency fibrillation) were constructed to perform hemodynamic analysis, and the computational results were compared. The results revealed that each characteristic phenomenon of AF influenced hemodynamics. Especially, atrial wall movement by high-frequency fibrillation had a large impact on the stagnation of blood flow. The relative residence time (RRT), which is an indicator of stagnation of blood flow, increased in the upper part of the LAA during AF. This result implies that there is a local thrombus-prone site in LAA when AF occurs.

1. Introduction

The left atrium (LA) is located at the upper dorsal part of the heart and has a characteristic part called the left atrial appendage (LAA), which bulges in the inner forward direction (Al-Saady et al., 1999). It pumps arterial blood from the four bilateral pulmonary veins (PVs) and ejects the blood toward the left ventricle (LV) through the mitral valve (MV) by both passive and active motions synchronized with ventricular expansion and contraction (Pagel et al., 2003). Atrial fibrillation (AF) is the most common arrhythmia which disrupts the movement of the LA (Iwasaki et al., 2011). The important characteristics of AF can be summarized as a lack of an active contraction of the LA (atrial kick) in late diastole and the occurrence of high-frequency fibrillation (>400 bpm) of the atrial wall. AF may cause no symptoms but is often associated with heart palpitation. Except for patients with severe underlying disease or hypofunction of LV contraction, aggressive treatments are not performed. However, it has been reported that thromboembolism derived from AF worsened the vital prognosis (Benjamin et al., 1998). An increase in the incidence of AF due to aging has also been suggested to be a cause of severe cerebral infarction (Wolf et al., 1991; Yamanouchi et al., 1989). Therefore, diagnosis, treatment, and management of AF are clinically important issues.

AF is diagnosed mainly by electrocardiogram (ECG). In order to diagnose the causes and complications of AF, morphological approach for entire heart, including LA and LAA, is conducted by means of computed tomography or ultrasound imaging, in addition to a blood test. On the other hand, there have been trials to utilize hemodynamic information on the LA obtained by phase-contrast magnetic resonance imaging (PC MRI) (Fluckiger et al., 2013; Fyrenius et al., 2001; Kilner et al., 2000) and ultrasonic measurement (Nakai et al., 2007; Nishimura et al., 1990; Park et al., 2013) for development of therapeutic strategy. Computational fluid dynamics (CFD) (Zhang and Gay, 2008) and particle image velocimetry (PIV)

* Corresponding author. Tel./fax: +81 22 217 5254.
E-mail address: funamoto@reynolds.ifs.tohoku.ac.jp (K. Funamoto).

http://dx.doi.org/10.1016/j.jbiomech.2014.12.025
0021-9290/

(Mouret et al., 2004) have also revealed morphological changes of vortices in the LV due to AF and stagnation of blood flow in the LAA leading to formation of thrombosis. However, though hemodynamics in LA during sinus rhythm and AF were qualitatively compared, no quantitative evaluations were conducted. Moreover, effects of each phenomenon caused by AF, i.e., the lack of an atrial kick and the occurrence of high-frequency fibrillation, on the blood flow field and hemodynamic stresses have not been completely understood.

In this study, effects of the above-mentioned two characteristics of AF on blood flow and hemodynamic parameters were quantitatively investigated. Hemodynamic analyses were performed using healthy and diseased LA models, and their computational results were compared.

2. Methods

2.1. Magnetic resonance imaging

This study was approved by the local ethics committees, and informed consent was obtained from the participating volunteer. First, for measurement of variation of the LA morphology, the heart of the 23-year-old healthy male volunteer was measured using a 1.5 T MRI scanner system (Achieva 1.5T, Philips Electronics, Holland) with a SENSE cardiac coil and a two-dimensional balanced turbo field echo at Miyagi Cardiovascular and Respiratory Center. Four chamber T1 weighted images were acquired on 12 slices at intervals of 5 mm with the following parameters: repetition time (TR), 3.3 ms; echo time (TE), 1.7 ms; flip angle (FA), 60°; field of view (FOV), 400 mm; and matrix size, 256 × 256 pixel. The image sets were obtained at 20 phases during the R–R interval (one cardiac cycle). Heart rate of the subject was 91 bpm (T=659 ms), so that 15 s was needed to obtain sequential images on one cross section. The total scan time was 6 min. Next, measurement of time-varying blood flow velocity in the LA was performed using a 1.5 T MRI scanner system (Excelart 1.5T, Toshiba Medical Systems, Japan) with a torso SPEEDER coil and phase shift magnetic resonance (MR) angiography at Tohoku Kosei Nenkin Hospital. All three velocity components were measured in the supine position in a four-chamber view. Thirteen slices were obtained at intervals of 5 mm, dividing one cardiac cycle into eight phases. The other parameters were set as follows: TR=24 ms, TE=10 ms, FA=20°, FOV=350 mm, matrix size=256 × 256 pixel, and VENC=1.0 m/s. The PC MRI data were obtained within 100 min. In each imaging, thoracic movement was reduced by breath-holding to suppress artifacts.

2.2. Left atrial model

As a basal model of computational models for numerical analysis, a three-dimensional (3D) morphology of the LA was reconstructed from a set of MR slice images in early diastole by using commercial software (Mimics 7.3, Materialise, Belgium). Fig. 1(a) shows the reconstructed left heart in stereolithography (STL) format: the red part is the LA, and the gray part is the LV. The LA has four PV inlets (PV1–PV4) and one MV outlet, and the LAA exists near PV3. Since the shape of the MV was not clearly identified in the MR images, it was replaced with a circle 24 mm in diameter (Ormiston et al., 1981). Cross-sectional areas of PVs and the MV in the computational model were as follows: PV1, 36.7 mm^2; PV2, 37.1 mm^2; PV3, 12.6 mm^2; PV4, 33.7 mm^2; and MV, 451.0 mm^2.

Deformation of the healthy LA model (HA model) in one cardiac cycle was obtained based on the location of the MV annulus in the MR slice images. As shown in Fig. 1(b), the xy coordinate system was defined with the origin at the upper-left position of the MR image. In addition, another $x'y'$ coordinate system was defined by setting the y' axis in the moving direction of the MV, and the origin was set at point (x_{org}, y_{org}) of little displacement. The positions of the left-side annulus of the MV were manually extracted on four of 12 MR slice images at each measured phase. The corresponding sequential positions at two different phases (see (x_{m1}, y_{m1}) and (x_{m2}, y_{m2}) in Fig. 1(b)) were then picked up and converted into the $x'y'$ coordinate system. For simplification, the right-side annulus of the MV was symmetrically determined by folding the one on the left side over the y'-axis. The movement of the lower part of the LA wall ($y' \geq 0$) in the y'-direction was computed with the assumption of a simple compression/extension, whereas that in the x'-direction was computed by linearly increasing the compression rate toward the MV. In contrast, the upper part of the LA ($y' < 0$) was fixed. Finally, a new morphology of the LA was obtained by inversely transforming the moved atrial wall in the $x'y'$ coordinate system into the xy coordinate system. Here, to continuously and smoothly change the LA morphology, a linear interpolation was applied between the slices. Moreover, an interpolation in the time domain was applied with a third-order spline interpolation based on the position of MV measured by MRI at 20 phases to divide one cardiac cycle into 200 computational time steps.

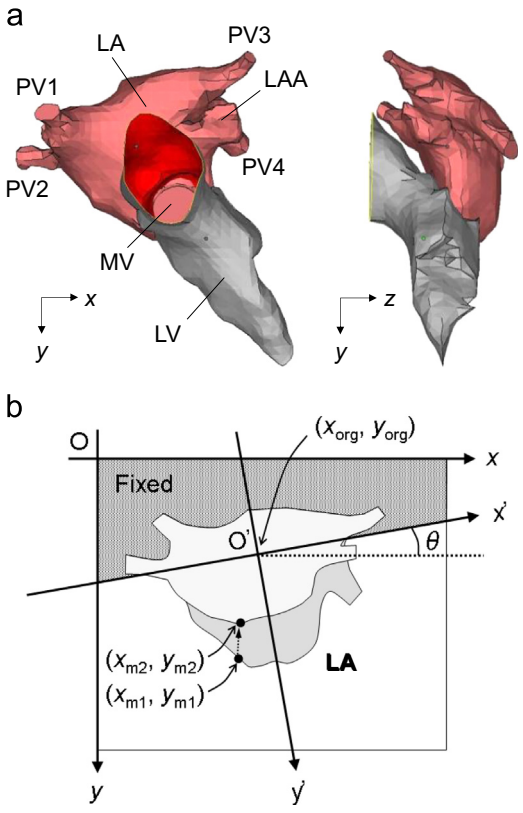

Fig. 1. A healthy left heart reconstructed from MRI: (a) 3D morphologies of the left atrium (LA, the red part) and the left ventricle (LV, the gray part), and (b) the definition of the coordinate systems. (For interpretation of the references to color in this figure legend, the reader is referred to the web version of this article.)

The MR slice image and the 3D morphology of the computational model are compared in Fig. 2 at four different time steps at t=0.033, 0.165, 0.330, and 0.494 s, corresponding to the computational time step of 10, 50, 100, and 150, respectively. The yellow outline superimposed on each MR image displays the corresponding cross section of the computational model. The blue and red cross sections in the computational models show PVs and the MV, respectively. The cross-sectional shapes of the HA model almost completely agree with those in the MR image though a gap is observed beneath the left PV at peak systole (t=0.330 s, see a white arrow). This implies the validity of the deformation estimated by the location of the MV annulus. Fig. 3 represents the variation of LA volume in the HA model, in which the MV closes in $t > 0.33$ s and an atrial kick showed a volume decrease in $0.25\ \text{s} \leq t \leq 0.33$ s. The time-varying volume of the LA was reproduced with the sufficiently small interval of time step with temporal interpolation of the MRI data.

Computational models mimicking AF were constructed based on the HA model since it was difficult to obtain MR slice images of an actual AF patient due to the limitation of time resolution of MRI. In this study, a model without an atrial kick (AF_0 model) and another model without an atrial kick and with high-frequency fibrillation (AF_1 model) were created as shown in Fig. 3. It is noted that the AF_0 model is different from the actual LA with AF, in which the lack of the atrial kick and high-frequency fibrillation occur simultaneously. However, the model was used as a comparative model to investigate the effects of each phenomenon of AF on hemodynamics. High-frequency fibrillation depends on the patient and the severity. In the AF_1 model, high-frequency fibrillation was modeled by a sine wave of 7.58 Hz (five times the heart beat) with an amplitude of 2.35% of the difference between the maximum and minimum volumes of the HA model.

2.3. Computational methods

The same algorithms and conditions were applied to computational analyses with the HA model and the AF_0 and AF_1 atrial fibrillation models. Density ρ and viscosity μ of blood were set within the normal range as 1050 kg/m^3 and 3.5×10^{-3} Pa s, respectively. Regarding boundary conditions, two conditions were switched between diastole and systole. In diastole ($0\ \text{s} \leq t \leq 0.33$ s), values of pressure at four inlets of PVs and one outlet of the MV were assumed to be constant at 10 mmHg and 8 mmHg, respectively (Smith and Kampine, 1980). Because of the pressure difference and the wall motion of the LA shown in Fig. 3, blood flowed through the LA. In systole ($0.33\ \text{s} < t \leq 0.66$ s), solid wall condition was assumed at the MV, which was close, while a constant pressure of 10 mmHg was maintained at

Please cite this article as: Koizumi, R., et al., Numerical analysis of hemodynamic changes in the left atrium due to atrial fibrillation. Journal of Biomechanics (2014), http://dx.doi.org/10.1016/j.jbiomech.2014.12.025